Supplemental Information

This document provides supplemental information on the methods and results of the current study,

Method

Participants

The final sample of the infant participants (N = 85, 39M / 46F) were from the Cryptosporidium burden study (CRYPTO) and the 115 (63M / 52F) toddlers were from the Performance of Rotavirus and Oral Polio Vaccines in Developing Countries study (PROVIDE). All infants and toddlers were born >= 34 gestational weeks. The participants had no history of neurological abnormalities or traumatic brain injury, no know genetic disorders, and no know visual or auditory delays or impairments. The original CRYPTO and PROVIDE cohorts each included 130 infants (56M / 74F) or children (72M / 58F). The average monthly household income for CRYPTO and PROVIDE cohorts is $187 (SD = 119) and $154 (SD = 107) respectively. The average HAZ, WAZ, and WHZ for the CRYPTO cohort were -1.13 (SD = .80), -.73 (SD = .95), .022 (SD = 1.01). The average HAZ, WAZ, and WHZ for the PROVIDE cohort were -1.42 (SD = .86), -1.42 (SD = 1.16), -.75 (SD = 1.04). Some participants (i.e., 45 out of 130 for CRYPTO and 15 out of 130) were excluded from the final sample of the current study because they had missing growth measures or EEG data, or their EEG data were excluded after artifacts rejection due to insufficient (< 80s out of 120s) clean data. The final infant (N = 85) and toddler (N = 115) samples were quite representative of the original CRYPTO and PROVIDE datasets in terms of sex, family income, and growth measures.

Ethical approval for the study was obtained from research review and ethics review committees at The International Centre for Diarrheal Disease Research, Bangladesh and Institutional Review Boards at Boston Children's Hospital and were in accordance with local guidelines and regulations. We have collected written consent forms from all families participated in the study.

EEG Data Collection and Processing

EEG was recorded from a 128-channel HydroCel Geodesic Sensor Net (HGSN) that was connected to a NetAmps 300 amplifier (Electrical Geodesic Inc., Eugene, OR) while children watched a screensaver with abstract shapes and soothing sounds for 2 mins. The EEG recording

was referenced online to a single vertex electrode. Channel impedance was kept below 100 kΩ and signals were sampled at 500 Hz.

EEG recordings were preprocessed using EEGLAB[1] and ERPLAB[2] toolboxes in MATLAB (R2017a, the Mathworks, Inc.). The continuous EEG data were filtered with an 8th order Butterworth band-pass filter with a pass band of 1 – 25 Hz. The low-pass cut-off was set to be below the gamma band to reduce the effect of the muscle- and movement-related artifacts on the children EEG data. The filtered data was then segmented into 1s epochs. The EEG epochs were inspected for artifacts using both absolute and stepwise algorithms (EEG > 100 μV, EEG < -100 μV, or ΔEEG > 100 μV within 100 ms with a 50 ms window step). Channel interpolation was conducted using the five closest channels if there were fewer than 18 (15%) electrodes that were missing or had bad data[3, 4]. Independent component analysis (ICA) was also conducted to remove components related to eye movements, blinks, and focal activity. The functions and algorisms in SASICA[5] and ADJSUT[6] were used to identify artificial components, and only those marked by both toolboxes were removed from the data. Each child must have at least 80 clean epochs (66.67%) to be included for further analyses. The number of artificial ICA components and the number of epochs included in the final analysis did not change as a function of the growth measures, *r*s < .1, *p*s >= .29.

EEG Functional Connectivity Analysis in the Source Space

The pipeline for the source-space functional connectivity analysis used in the current study was illustrated in Supplemental Figure 1 (also see[7]). Cortical source reconstruction was conducted for the scalp EEG data with the Fieldtrip toolbox[8]. Realistic head models were created for both 6- and 36-month-old cohorts using age-appropriate average MRI templates selected from the Neurodevelopmental MRI Database[9, 10]. Anatomical MRI templates were segmented into component materials, and a forward model was created for each age group using the Finite Element Method (FEM) with the gray matter being used as source volumes (5 mm grids). Age-appropriate skull conductivity values (0.066 $\Omega \cdot m^{-1}$ for the 6-month model and 0.036 $\Omega \cdot m^{-1}$ for the 36-month model) were used to build the models[11]. The forward model was then used to estimate the lead field matrix and the spatial filter matrix, i.e., the inverse of the lead field matrix.

Distributed source reconstruction of the EEG time-series was conducted with the exact-LORETA (eLORETA[12]) as the constraint for inverse modeling. The source volumes were

segmented into 48 cortical regions of interest (ROIs) using the LPBA40 brain atlas[13]. The reconstructed time-series in the source volumes surrounding the centroid of each ROI were averaged to represent the source activation for each ROI[14].

Functional connectivity analysis was conducted with the source-space time-series for the 48 cortical ROIs. Given the dramatic changes in the peak frequency of different frequency rhythms in the first few years of life (Marshall et al., 2002; Perone et al., 2018), age-appropriate frequency bands were used for the theta (6 mos: 3 – 6 Hz; 36 mos: 4 – 7 Hz), alpha (6 mos: 6 – 9 Hz; 36 mos: 7 – 11 Hz), and beta1 (6 mos: 9 – 15 Hz; 36 mos: 11 – 15 Hz) rhythms.

The functional connectivity between ROIs in different frequency bands was estimated with weighted phase lag index (wPLI[15]), a measure that weights the phase differences according to the magnitude of the leads and lags so that phase differences close to zero generated by noise perturbations would only have a marginal contribution to the results. In addition, random permutation of trials was applied to get rid of the effect of number of observations (trials) on the wPLI estimation[15], as the number of trials did differ between individuals. In specific, 80 trials were randomly selected from all the trials (varying between 80 and 120) to calculate the wPLI value between ROIs. This procedure was repeated for 50 times and the average wPLI value was calculated. Functional connectivity analysis resulted in 48 x 48 weighted adjacency matrices, with each element in the matrix representing the connectivity between a pair of ROIs. The Fisher's r-to-z transformation was applied to the values in the matrices to improve the normality of their distribution. A sparsity threshold of .2 (20%) was applied to the matrices to retain the strong and eliminate the weak or noise connections, as well as to keep the same number of connections across matrices[16]. Analyses were also done with thresholds of .3 and .1 to exclude the possibility that the results of the experiment are driven by the choice of network thresholds, and similar results were obtained across thresholds.

Results

Model Fit in SEM Analysis

SEM analysis was conducted to estimate prospective relationships between growth measures and brain functional connectivity, and the prospective relationship between brain functional connectivity and later cognitive outcomes. We explored both direct as well as indirect effects (via brain connectivity) of growth measures on later cognitive outcomes. The model fits in the SEM analyses for the three growth measures (i.e., three models) are reported as following:

the “HAZ model”: $\chi^2(1) = 1.545$, P= .214; CFI= .985; SRMR=.027; RMSEA = .069; the “WAZ model”: $\chi^2(1) = 1.245$, P= .265; CFI= .994; SRMR=.023; RMSEA = .046; and the “WHZ model”: $\chi^2(1) = .928$, P= .336; CFI= 1.00; SRMR=.021; RMSEA < .001.

Validation Analysis of EEG Functional Connectivity Estimated with iCOH

The estimation of EEG functional connectivity could be affected by the algorisms or methods used to calculate the phase-based relationship between two time series[17]. Therefore, we further estimated brain functional connectivity using the imaginary part of the coherency (iCOH[18]). Correlations between growth measures and functional connectivity estimated with iCOH were calculated to validate the results from using the wPLI method presented in the results section of the manuscript. The analysis with functional connectivity estimated with iCOH yielded very similar results to those with wPLI, i.e., there were negative correlations between the growth measures and brain functional connectivity in the low-beta band. Growth measures were negatively correlated with the overall brain functional connectivity in the low-beta band estimated with the iCOH method for the 36-month-old cohort: HAZ ($r = -.22$, $p = .017$), WAZ ($r = -.28$, $p = .0026$), and WHZ ($r = -.25$, $p = .0061$).

Supplemental Figure 1. *The pipeline for EEG functional connectivity analysis in the source space used in the current study.*

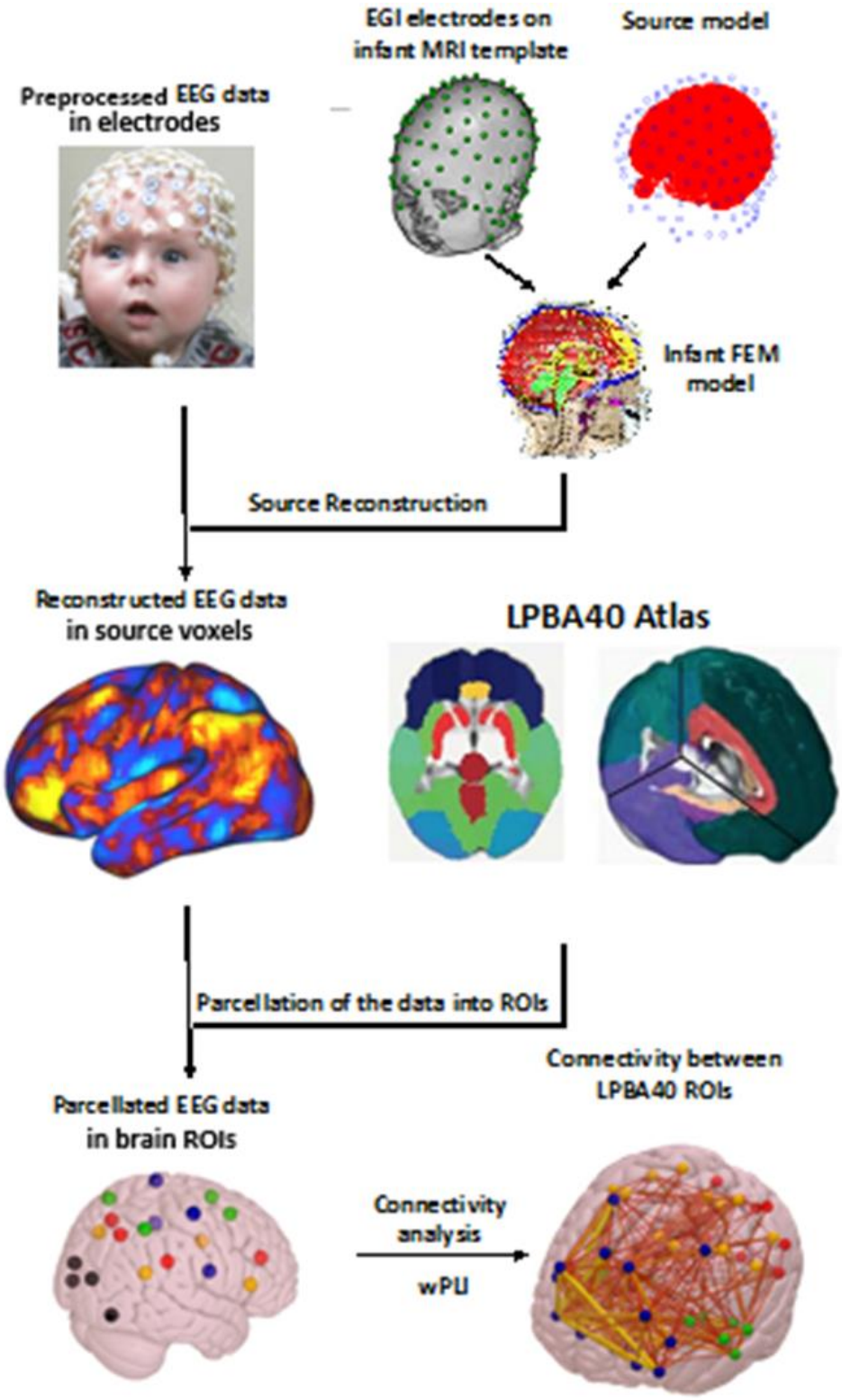

References in Supplemental Information

1. Delorme A, Makeig S. EEGLAB: an open source toolbox for analysis of single-trial EEG dynamics including independent component analysis. J Neurosci Methods. 2004;134(1):9-21.
2. Lopez-Calderon J, Luck SJ. ERPLAB: an open-source toolbox for the analysis of event related potentials. Front Hum Neurosci. 2014;8.
3. Luyster RJ, Powell C, Tager-Flusberg H, Nelson CA. Neural measures of social attention across the first years of life: characterizing typical development and markers of autism risk. Dev Cogn Neurosci. 2014;8:131-43.
4. Righi G, Westerlund A, Congdon EL, Troller-Renfree S, Nelson CA. Infants' experience-dependent processing of male and female faces: insights from eye tracking and event-related potentials. Dev Cogn Neurosci. 2014;8:144-52.
5. Chaumon M, Bishop DV, Busch NA. A practical guide to the selection of independent components of the electroencephalogram for artifact correction. Journal of neuroscience methods. 2015;250:47-63.
6. Mognon A, Jovicich J, Bruzzone L, Buiatti M. ADJUST: An automatic EEG artifact detector based on the joint use of spatial and temporal features. Psychophysiology. 2011;48(2):229-40.
7. Xie W, Mallin BM, Richards JE. Development of brain functional connectivity and its relation to infant sustained attention in the first year of life. Dev Sci. 2018:e12703.
8. Oostenveld R, Fries P, Maris E, Schoffelen JM. FieldTrip: Open source software for advanced analysis of MEG, EEG, and invasive electrophysiological data. Computational intelligence and neuroscience. 2011;2011:156869.
9. Richards JE, Sanchez C, Phillips-Meek M, Xie W. A database of age-appropriate average MRI templates. NeuroImage. 2016;124:1254-9.
10. Richards JEX, W. Brains for all the ages: Structural neurodevelopment in infants and children from a life-span perspective. In: Benson J, editor. Adv Child Dev Behav. 48. Philadephia, PA: Elsevier; 2015. p. 1-52.
11. Hamalainen JA, Ortiz-Mantilla S, Benasich AA. Source localization of event-related potentials to pitch change mapped onto age-appropriate MRIs at 6 months of age. NeuroImage. 2011;54(3):1910-8.
12. Pascual-Marqui RD, Lehmann D, Koukkou M, Kochi K, Anderer P, Saletu B, et al. Assessing interactions in the brain with exact low-resolution electromagnetic tomography. Philosophical transactions Series A, Mathematical, physical, and engineering sciences. 2011;369(1952):3768-84.
13. Shattuck DW, Mirza M, Adisetiyo V, Hojatkashani C, Salamon G, Narr KL, et al. Construction of a 3D probabilistic atlas of human cortical structures. NeuroImage. 2008;39(3):1064-80.
14. Hillebrand A, Barnes GR, Bosboom JL, Berendse HW, Stam CJ. Frequency-dependent functional connectivity within resting-state networks: An atlas-based MEG beamformer solution. NeuroImage. 2012;59(4):3909-21.
15. Vinck M, Oostenveld R, van Wingerden M, Battaglia F, Pennartz CM. An improved index of phase-synchronization for electrophysiological data in the presence of volume-conduction, noise and sample-size bias. NeuroImage. 2011;55(4):1548-65.
16. Bathelt J, O'Reilly H, Clayden JD, Cross JH, de Haan M. Functional brain network organisation of children between 2 and 5 years derived from reconstructed activity of cortical sources of high-density EEG recordings. NeuroImage. 2013;82:595-604.
17. Mahjoory K, Nikulin VV, Botrel L, Linkenkaer-Hansen K, Fato MM, Haufe S. Consistency of EEG source localization and connectivity estimates. NeuroImage. 2017;152:590-601.
18. Nolte G, Bai O, Wheaton L, Mari Z, Vorbach S, Hallett M. Identifying true brain interaction from EEG data using the imaginary part of coherency. Clinical Neurophysiology. 2004;115(10):2292-307.